



Article

Using Energy Conservation-Based Demand-Side Management to Optimize an Off-Grid Integrated Renewable Energy System Using Different Battery Technologies

Polamarasetty P Kumar, Akhlaqur Rahman, Ramakrishna S. S. Nuvvula, Ilhami Colak, S. M. Muyeen, Sk. A. Shezan, G. M. Shafiullah, Md. Fatin Ishraque, Md. Alamgir Hossain, Faisal Alsaif et al.

Special Issue

Optimized Design of Hybrid Microgrid








Edited by

Dr. Arefin Shezan and Dr. Mohammed Nazmus Shakib



Article

Using Energy Conservation-Based Demand-Side Management to Optimize an Off-Grid Integrated Renewable Energy System Using Different Battery Technologies

Polamarasetty P Kumar ¹, Akhlaqur Rahman ^{2,*} , Ramakrishna S. S. Nuvvula ^{1,3} , Ilhami Colak ⁴, S. M. Mueen ⁵ , Sk. A. Shezan ^{2,6} , G. M. Shafiullah ⁶ , Md. Fatin Ishraque ⁷ , Md. Alamgir Hossain ⁸ , Faisal Alsaif ⁹  and Rajvikram Madurai Elavarasan ¹⁰ 

¹ Department of Electrical and Electronics Engineering, GMR Institute of Technology, Rajam 532127, India; praveenkumar.p@gmrit.edu.in (P.P.K.); nramkrishna231@gmail.com (R.S.S.N.)

² School of Electrical Engineering and Industrial Automation, Engineering Institute of Technology, Melbourne Campus, Melbourne, VIC 3001, Australia; shezan.ict@gmail.com or shezan.arafin@eit.edu.au

³ Department of Electrical and Electronics, NMAM Institute of Technology, Nitte, Karkala 574110, India

⁴ Department of Electrical and Electronics Engineering, Faculty of Engineering and Architecture, Nisantasi University, Istanbul 34100, Turkey; ilhcol@gmail.com

⁵ Department of Electrical Engineering, Qatar University, Doha 2713, Qatar; sm.mueen@qu.edu.qa

⁶ School of Engineering and Energy, Murdoch University, Murdoch, WA 6150, Australia; gm.shafiullah@murdoch.edu.au

⁷ Department of Electrical and Electronics Engineering, Pabna University of Science and Technology, Pabna 6600, Bangladesh; fatineeruet@gmail.com

⁸ Queensland Micro and Nano-Technology Centre, Griffith University, Nathan, QLD 4113, Australia; mdalamgir.hossain@griffith.edu.au

⁹ Department of Electrical Engineering, College of Engineering, King Saud University, Riyadh 11421, Saudi Arabia; faalsaif@ksu.edu.sa

¹⁰ Research & Development Division (Power & Energy), Nestlives Private Limited, Chennai 600091, India; rajvikram@nestlives.com

* Correspondence: akhlaqur.rahman@eit.edu.au



Citation: Kumar, P.P.; Rahman, A.; Nuvvula, R.S.S.; Colak, I.; Mueen, S.M.; Shezan, S.A.; Shafiullah, G.M.; Ishraque, M.F.; Hossain, M.A.; Alsaif, F.; et al. Using Energy Conservation-Based Demand-Side Management to Optimize an Off-Grid Integrated Renewable Energy System Using Different Battery Technologies. *Sustainability* **2023**, *15*, 10137. <https://doi.org/10.3390/su151310137>

Academic Editors: George Kyriakarakos and Elena Lucchi

Received: 8 March 2023

Revised: 6 June 2023

Accepted: 12 June 2023

Published: 26 June 2023



Copyright: © 2023 by the authors. Licensee MDPI, Basel, Switzerland. This article is an open access article distributed under the terms and conditions of the Creative Commons Attribution (CC BY) license (<https://creativecommons.org/licenses/by/4.0/>).

Abstract: Rural electrification is necessary for both the country's development and the well-being of the villagers. The current study investigates the feasibility of providing electricity to off-grid villages in the Indian state of Odisha by utilizing renewable energy resources that are currently available in the study area. However, due to the intermittent nature of renewable energy sources, it is highly improbable to ensure a continuous electricity supply to the off-grid areas. To ensure a reliable electricity supply to the off-grid areas, three battery technologies have been incorporated to find the most suitable battery system for the study area. In addition, we evaluated various demand side management (DSM) techniques and assessed which would be the most suitable for our study area. To assess the efficiency of the off-grid system, we applied different metaheuristic algorithms, and the results showed great promise. Based on our findings, it is clear that energy-conservation-based DSM is the ideal option for the study area. From all the algorithms tested, the salp swarm algorithm demonstrated the best performance for the current study.

Keywords: integrated renewable energy; off-grid; optimization techniques; demand-side management; different batteries; microgrid

1. Introduction

In isolated rural locations, renewable energy sources, such as solar and biomass, are being increasingly used to meet electricity demands. Many off-grid areas cannot access grid-connected power supply, but these regions can take advantage of the readily available RE sources to power their homes and businesses. Due to the fluctuating nature of major renewable energy sources that vary depending on the time of day and season, an off-grid

electric grid that is based on renewable energy cannot guarantee an uninterrupted power supply [1]. Therefore, an efficient Energy Management Plan is essential for a reliable off-grid electricity supply, requiring the combination of one or two renewable energy sources with a battery storage system. The microgrid must be sized appropriately; if undersized, power losses will occur, and if oversized, the development costs may be excessive and lead to energy waste. To ensure the RE-based microgrid's benefits are fully realized, an efficient Energy Management Plan is vital [2].

This study conducted a techno-economic analysis of three different types of batteries, including LA, Li-Ion, and Ni-Fe, with a particular focus on the use of the LA battery technology in developing countries, such as India, Pakistan, Bangladesh, and Sri Lanka, due to its lower cost compared to other options. Although it has certain drawbacks in terms of its lifespan and durability, these batteries are still being used to provide electricity to remote rural areas in these countries. The life of these batteries is shorter than other types, and their longevity is dependent on the temperature they are in. This means that they need to be replaced every three to five years, which can present a challenge in more remote locations due to transportation difficulties. Thus, it is important to consider the technical and economic characteristics of these batteries, such as their lifespan, durability, round trip efficiency, high operating temperature capability, capital cost, replacement expense, and annual O&M cost, prior to initiating a project [3].

In order to tackle the issues discussed previously, this study proposes the use of Ni-Fe batteries. Although they may not be widely known, they are the most efficient and durable battery technology available today, making them suitable for off-grid solar and other green energy initiatives. Historically, Ni-Fe batteries have a 100-year track record. In the early 1900s, Thomas Edison patented and developed them to be "stronger than lead-acid batteries". The first electric car was also equipped with this type of battery in the early 1910s. They were not used as starting batteries for cars but gained popularity in the 20th century for forklifts, railroad applications, and standby power. In the 21st century, these batteries are being utilized again, this time in renewable energy applications due to their durability, long lifespan, and incredible robustness. Unlike most other batteries, the life cycle of the Ni-Fe batteries is not impacted by their depth of discharge (DOD). This allows users to discharge them to 80% of their capacity without significantly reducing their battery life. By contrast, over-discharging an LA battery even once can result in a drastically reduced lifespan. The same cannot be said for Ni-Fe batteries, as their life expectancy is unaffected by discharging beyond 80%, and they can withstand overcharging without compromising longevity [3].

Optimization problems and theories encompass a wide variety of applied mathematics. Discovering the optimal size of a hybrid renewable energy system is a type of constrained optimization issue, which entail one or a few objectives in addition to integral or distinct variables as well as numerous linear or nonlinear limits. The renewable sizing issue is believed to have multiple local optimum solutions and a solitary global best optimal solution. Consequently, exploring the global optimal result is the most essential point to take into account [4].

Studies into the field of microgrid sizing have been reported in the literature, which can be categorized into three groups: software tools (such as HOMER, RETScreen, HOGA, and IHOGA) [5]; deterministic methods (including iterations, numerical, linear programming, graphical construction, probabilistic and analytical); and metaheuristic algorithms (e.g., GA, PSO, GOA, and GWO) [4]. Of the three, software tools are user-friendly but limited in their capacity to pick components. Deterministic methods work efficiently but may be stuck at local optima. Several times, global best optimal solutions may be unable to be reached [2].

Over the past ten years, scientists have developed and used various metaheuristic algorithms for the purpose of microgrid sizing. GA, PSO, and DE, for example, are popular methods among computer scientists and experts from various fields, as they are flexible, offer a solution that surpasses that of deterministic algorithms, and avoid local optima traps [4]. Despite the fact that a particular metaheuristic algorithm can

yield optimal results for one specific objective function, the same algorithm will create substandard results for other objectives based on the no free lunch theorem [6]. Motivated by the aforementioned factors, scientists have been exploring novel algorithms to address microgrid sizing problems [4].

In remote communities, poor load demand coordination and irregular renewables can lead to higher energy costs. To address this issue, the power system industry has implemented various demand-side management (DSM) strategies such as “load shaping”, “load shifting”, “energy conservation”, “load building”, and “peak clipping” (see Figure 1). These strategies can help to reduce energy costs by improving the coordination of load demand and incorporating renewable energy sources more effectively [7] as follows:

- i. **Peak clipping:** Its purpose is to reduce the strain on energy systems during peak demand periods. This is typically achieved by limiting the use of appliances during peak hours or by offering customers incentives to shift their energy consumption away from peak times;
- ii. **Valley filling:** The aim of valley filling is to maximize the utilization of facilities by promoting energy consumption during off-peak hours. To achieve this, governments can incentivize customers to schedule such activities as charging and loading during off-peak times. By doing this, customers will be able to take full advantage of available resources, resulting in more efficient use of energy;
- iii. **Load shifting:** To reduce overall energy consumption, load shifting from peak to off-peak times is recommended. Customers can store thermal heat during the off-peak hours, which can then be used to maintain a comfortable temperature throughout the day. Furthermore, household chores, such as laundry and dishwashing, can be completed at night to avoid peak loading;
- iv. **Energy conservation:** Its goal is to reduce energy consumption by investing in more energy-efficient devices. This can help lower load demand, thus leading to more efficient energy use overall;
- v. **Load building:** Smart grids enable the use of load building and flexible loads through the improved network connection. This, in turn, increases the grid’s responsiveness through improved load sharing and the application of energy storage systems;
- vi. **Flexible load shape:** By adjusting the flexible load demand, the reliability conditions necessary for system reliability can be determined, thus improving the system’s reliability.

In rural areas, the load consumption pattern of most people remains fairly consistent throughout the day. Since priority loads, such as lamps, fans, and televisions, are usually used in the evening, and their usage cannot be altered, rural off-grid villagers cannot participate in peak clipping or load shifting at this time. However, Energy-Conservation-based Demand Management can still help reduce peak loads without resorting to peak clipping or load shifting.

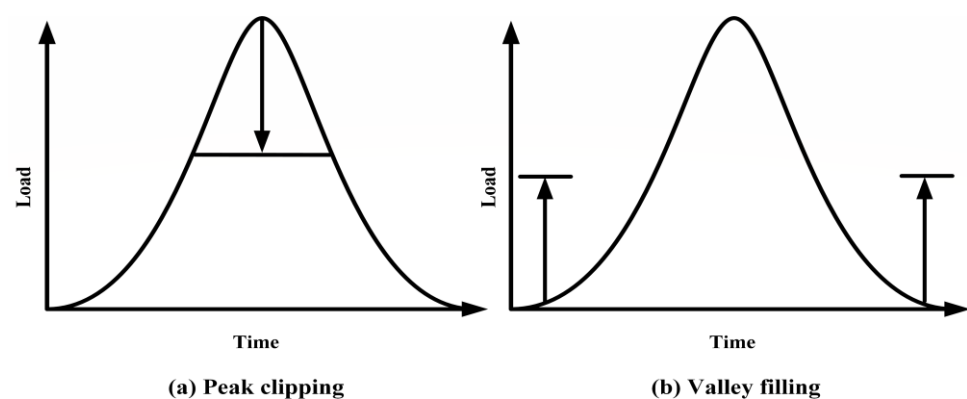


Figure 1. Cont.

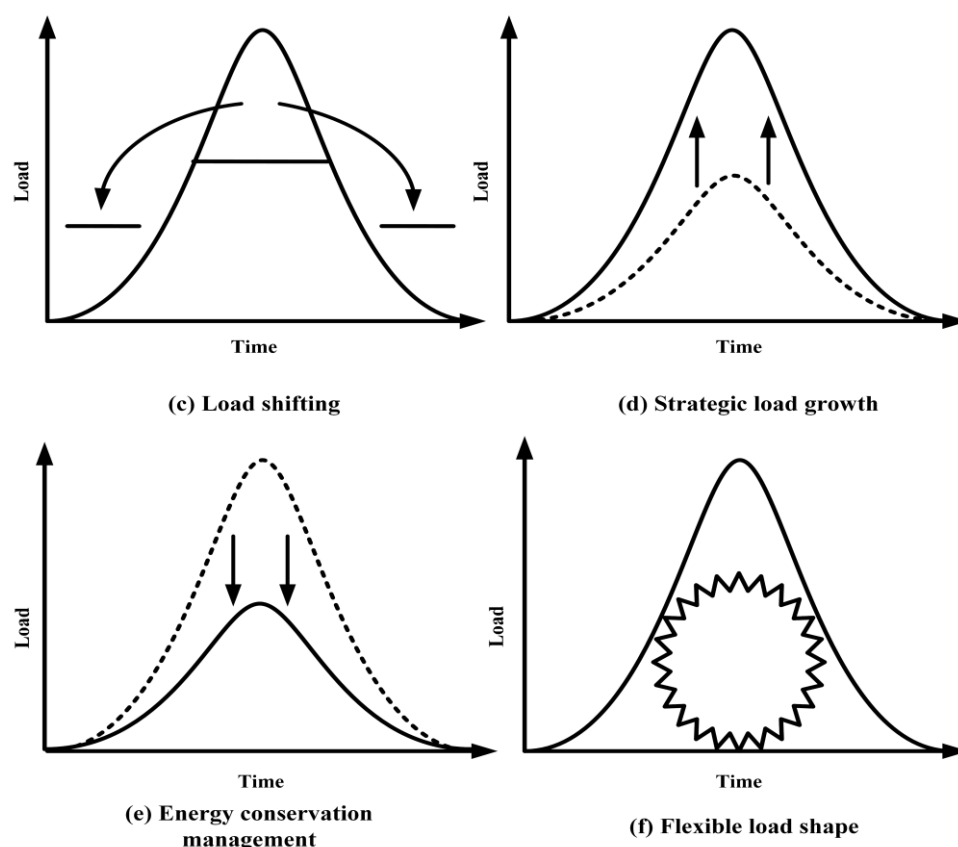


Figure 1. All types of demand-side management.

1.1. The Literature Review

- Alpesh and Sunil [1] utilized a combination of PV/Wind Turbine (WT)/Biomass Generator (BMG)/Biogas Generator (BGG)/LA battery technology to electrify hamlets with 123 households located on the border of India's Gujarat and Rajasthan states and analyzed the optimal component selection using multi-variable linear regression technique along with the gradient descent (MVLRT-GD) algorithm and particle swarm optimization (PSO) to determine the optimal results;
- Ramesh and Saini [8] conducted a study that assessed the feasibility of PV/WT/Micro Hydro Power Plant (MHP)/Diesel Generator (DG)/Battery (BAT) configurations with LA and Li-Ion battery technologies for off-grid un-electrified villages in Chikmagalur district in India. They used HOMER Pro[®] software to evaluate three different dispatch strategies and found that the Li-Ion-battery-based system with a combined dispatch strategy provided the lowest net present cost (NPC) and cost of energy (COE) compared to the cycle charging and load-following strategy-based systems using the LA battery technology;
- Haein and Tae [9] studied the most cost-effective way to electrify an off-grid rural area in Myanmar by using PV/DG/BAT configuration with both LA and Li-Ion battery technologies. They used the HOMER Pro[®] software tool to minimize the NPC of the system and determined that using the LA battery technology provided the most optimal results;
- Kaabeche and Bakelli [10] evaluated the PV/WT/BAT system with LA, Li-Ion, and nickel-cadmium battery technologies in Adrarin province, Algeria. They applied various optimization algorithms, such as GWO, ALO, Krill Herd, and JAYA, to minimize the electricity cost of the system and concluded that LA battery-based configuration with the JAYA algorithm was the most optimal solution, followed by the Li-Ion and Ni-Cd batteries;

- Sarah et al. [11] examined the PV/WT/DG/BAT system for Dodoma, Tanzania, with both LA and Li-Ion battery technologies to identify the most cost-efficient configuration. These researchers found that Li-Ion battery configuration with a genetic algorithm provided the lowest cost of energy (COE);
- Chong Li et al. [12] conducted a study of the WT/DG/BAT system for 280 off-grid households in Gansu province, China, with LA, Li-Ion, and Zinc–Bromine (ZB) battery technologies. They used the HOMER Pro[®] software tool to determine the optimal option and found that the ZB battery technology provided the optimal results;
- Muhammad Fahad Zia et al. [7] examined the use of a microgrid for remote area applications, such as oceanic islands, specifically in the context of Ouessant Island in Brittany, France. The microgrid consists of a PV system, tidal turbine, diesel generator, and Li-Ion battery, and the economic operation of the system is achieved by taking into account various factors, such as battery degradation cost, leveled costs of energy, operating and emission costs of the diesel generator, and network constraints;
- George K. Farinis and Fotios D. Kanellos [13] proposed an energy management system for microgrids and building prosumers using a multi-agent system, particle swarm optimization, and thermal and electrical models. It allows for optimal operation scheduling in grid-connected and autonomous operational modes and can result in cost savings of around 11%. Simulation results demonstrate its effectiveness in meeting a large number of operation and technical constraints;
- Vasileios Boglou et al. [14] used a decentralized energy management system based on multi-agent systems, which was developed for the efficient charging of electric vehicles. This approach leads to a significant reduction in investment costs, peak load, and load variances. Furthermore, it increases the total amount of chargeable EVs. This novel charging management system offers an intelligent approach to the islanding of distribution grids with high penetration of electric vehicles by offering operational and financial benefits;
- Eliseo Zarate-Perez et al. [15] used a systematic and bibliometric approach to evaluate the performance and challenges of integrating battery energy-storage systems into microgrids. This review finds that optimization methods and cost-benefit analysis are key elements for developing an optimal battery energy-storage system. Other considerations include factors, such as reliability, battery technology, power quality, frequency variations, and environmental conditions. Overall, economic factors are the biggest challenges for battery energy-storage systems;
- Vasileios Boglou et al. [16] proposed a distributed optimal small-scale PV energy-system-sizing strategy for residential distribution grids that takes into account individual energy needs and EV charging. Fuzzy cognitive maps theory is used to address the correlation between individual energy parameters and RES characteristics. The optimization results showcase that the adopted hybrid approach can reduce energy costs significantly, with no need for expansion of the utility network. Thus, EV charging through residential RES can become a viable option;
- Dimitrios Rimpas et al. [17] reviewed various motor technologies available for use in electric vehicles, such as brushless motors, synchronous reluctance, and induction motors. By taking into account eleven criteria, such as power density and regenerative braking efficiency, the motors are classified in terms of their ability to function in hybrid energy-storage systems to maximize efficiency and sizing. It is concluded that permanent magnet motors and induction motors are the most suitable for such applications, with the synchronous reluctance motor offering superior performance when it comes to the key factors impacting the system;
- Shih-Chieh Huang et al. [18] integrated a structural equation model (SEM) and fuzzy cognitive map (FCM) to analyze the mutual relationship between the various elements influencing the development of wind power. Results suggest that “policy” is the main obstacle to development, and management strategies should focus on the “technology”

and “environment” in the short term and consider “social” factors in the mid-term, with a focus on “policy” in the long-term;

- Christos-Spyridon Karavas et al. [19] proposed a decentralized energy management system for an autonomous polygeneration microgrid topology. A decentralized architecture offers advantages, such as greater chances of partial operation in cases of malfunctions, in comparison with a centralized system. The multi-agent system based on fuzzy cognitive maps was explored for their implementation and compared to an existing centralized energy management system in terms of technical performance, financial efficiency, and operational simplicity. The results showed similar technical performance between the two systems, along with advantages in financial and operational terms for the decentralized system;
- Konstantinos Kokkinos et al. [20] proposed a semi-quantitative assessment of biowaste-based energy transition by engaging stakeholders. To achieve this, a decision support system (DSS) and a fuzzy cognitive map (FCM) are proposed to evaluate the interplay of local and sectoral low-carbon actions. A use case study of a Greek region is potentially employed to analyze the effect of energy provision on urbanization and the influence of actors on decision-making related to low-carbon policies. The proposed decision-making tool utilizes analytics, optimization algorithms, and surveys to guide competent authorities to sustainable energy transitioning toward decarbonization;
- Lucchi E.’s design policy-related requirements that protect existing history and cultural values are essential for the successful integration of such renewable energy sources as photovoltaics into the built environment. As part of this process, he conferred with heritage authorities to learn about the most up-to-date standards, as well as the benefits and cons of the potential integration of solar energy and other renewable sources into the cultural heritage sites. Proper implementation of this strategy can improve clean and integrated energy production, which, in turn, can help mitigate climate change and fulfil today’s energy demands;
- Lucchi, E., Baiani, S., and Altamura, P. studied to aid in the design and construction of historically significant buildings that incorporate active solar technology, such as photovoltaic and solar thermal systems, by providing a classification system for international norms. By analyzing and comparing recurring criteria and recommendations from 44 international guidelines, it develops and identifies shared-design requirements for the integration of various active solar technologies and works to create a shared vocabulary to promote their adoption. They also look at how incorporating active solar technologies can increase a building’s market value, improve occupants’ quality of life, and reduce energy consumption while also positively supporting energy transition and climate change mitigation;
- Lucchi E.’s study shows that applied to historic buildings, they can cause significant conservation problems that endanger the buildings’ cultural significance, biodiversity, traditional appearance, and even the materials themselves. Based on a survey of the literature from 2020 to 2023, this study provides an up-to-date summary of the use of such renewable energy sources as solar, wind, geothermal, and bioenergy to preserve historic buildings. Acceptability, design requirements, and cutting-edge technologies are discussed, with examples from real-world applications. The compatibility of wind turbines with their natural and cultural surroundings and municipal rules is crucial to the widespread adoption of wind energy in historical sites. Heating and cooling systems, among other geothermal energy uses, have been effectively incorporated in both old and new buildings.

1.2. Research Gaps Identified

- From the research in the Indian context, using lithium-ion (Li-Ion), lead–acid (LA), and nickel–iron (Ni–Fe) batteries for the off-grid microgrids has not been thoroughly explored. To gain an understanding of the advantages of these technologies in off-grid microgrids, further research is necessary. This should include an analysis of cost-

effectiveness, reliability, long-term performance, environmental impact, and a cost-benefit assessment. Additionally, safety, usability, scalability, and potential integration with other energy sources should also be considered;

- Further, the majority of studies carried out a techno-economic feasibility analysis with one or two types of battery technologies to provide a continuous power supply. This often fails to take into account the unique requirements and characteristics of different battery technologies. Given that lithium-ion (Li-Ion), lead-acid (LA), and nickel-iron (Ni-Fe) each have distinct advantages and disadvantages, it is important to explore the potential for utilizing these technologies for the off-grid microgrids in order to create an optimal balance between cost, performance, and reliability. Furthermore, there is a need for further research into the design of these combinations and their potential for scalability and integration with other energy sources;
- Further research can be conducted to compare the proposed algorithm with other algorithms in terms of robustness, efficiency, and scalability. Such studies would help identify the best algorithms for different conditions, such as complexity, grid constraints, load profiles, and cost considerations. Additionally, other approaches, such as meta-heuristics and optimization techniques, could also be applied to the off-grid microgrid-sizing problem. This would enable a more comprehensive comparison between various algorithms in terms of performance and implementation;
- Demand side management (DSM) strategies have the potential to play a major role in achieving better energy balance and overall efficiency of the off-grid microgrids. However, there is still a need for more studies to explore the potential benefits of different DSM approaches for off-grid microgrids. Research should focus on the assessment of individual DSM techniques, such as time-of-use pricing, demand-response programs, dynamic pricing, and the potential for their combinations with other distributed energy resources, such as solar PV, storage, and wind turbines. Further, there is an urgent need to investigate the potential of energy-conservation DSM strategies for off-grid microgrids, such as energy-efficiency measures, demand management, and load shifting. Such research could help to identify cost-effective approaches that can improve the operational efficiency and overall economic viability of the off-grid microgrids.

1.3. *Novelties of This Article*

- The techno-economic reliability of providing energy to five off-grid communities in the Rayagada region of Odisha state in India was studied, leveraging existing renewable energy sources in the area, such as solar and biomass. Furthermore, a novel method of combining these two energy sources was proposed to create a reliable energy system that optimizes cost-effectiveness and maximizes sustainability. This new approach could be applied to other off-grid communities to provide secure and affordable energy access;
- Six specific configurations are modeled by the available RE sources and suggested batteries "PV/BMG/LA@70% DOD, PV/BMG/LA@80% DOD, PV/BMG/Li-Ion@50% DOD, PV/BMG/Li-Ion@70% DOD, PV/BMG/Li-Ion@80% DOD, and PV/BMG/Ni-Fe@80% DOD" with their varying depths of discharge to figure out which configuration will provide the most reliable power supply;
- To identify the most reliable power supply, six specific configurations of renewable energy sources and suggested batteries have been modeled, with varying depths of discharge. The configurations are PV/BMG/LA@70% DOD, PV/BMG/LA@80% DOD, PV/BMG/Li-Ion@50% DOD, PV/BMG/Li-Ion@70% DOD, PV/BMG/Li-Ion@80% DOD; and PV/BMG/Ni-Fe@80% DOD;
- This research has presented a unique solution for solving optimization problems—the salp swarm algorithm. This algorithm is a novel metaheuristic algorithmic approach that does not rely on predetermined parameters. Furthermore, the results obtained from testing this algorithm demonstrate superior performance to existing optimization algorithms across various metrics. This algorithm shows a high degree of robustness

and convergence efficiency compared to eight other algorithms, including the particle swarm optimization (PSO) [21], differential evolutionary algorithm (DE) [22], genetic algorithm (GA) [23], ant lion optimization (ALO) [24], grasshopper optimization algorithms (GOA) [25], grey wolf optimization (GWO) [26], moth flame optimization (MFO) [27], and dragonfly algorithm (DA) [28]. It is clear that the salp swarm algorithm is a reliable and effective algorithm for solving optimization problems and can be used to significantly improve the performance of optimization solutions;

- This research not only explored various demand-side management techniques but also implemented energy-conservation-based demand-side management for the current study area. The results were impressive, as it effectively reduced peak-load demands and improved customer satisfaction while providing a reliable and cost-effective power system. Furthermore, with these successes in mind, this strategy can be applied to other areas in need of a demand-side management technique, allowing for a larger-scale approach to energy conservation and security. As such, this method proves to be an innovative, effective, and much-needed solution for meeting the growing energy requirements.

2. Development of the Integrated Renewable Energy System

In order to reap the numerous benefits of an Integrated Renewable Energy System (IRES) in isolated rural communities, a comprehensive, strategic plan should be developed and followed. Such a plan should involve extensive research and analysis of the local environment, resources, and infrastructure, as well as the development of detailed goals and objectives. It should also incorporate detailed implementation strategies, including the selection of the right technologies, equipment, and services for the region and a timeline for the IRES installation. By properly planning and executing such a system, these remote communities can gain access to clean, renewable energy and benefit from sustainable energy sources. In order for an Integrated Renewable Energy System to be successfully implemented in isolated rural areas, a deliberate approach must be taken. To ensure the successful installation and functioning of the IRES, a carefully developed and executed plan is necessary, the steps of which are listed as follows:

Step 1—Study-area identification

The research area, located at $19^{\circ}37'16.6944''$ N and $83^{\circ}29'50.6688''$ E, is situated 206 m above sea level in the Muniguda of Rayagada region in the Indian state of Odisha (as depicted in Figure 2). This area consists of 5 un-electrified communities with 266 homes and a total population of 1213 people who struggle to access reliable electricity.

Step 2—Estimation of electrical energy demand

This study examined the load demands of three different types of appliances: low-power-rated appliances of high cost (LPRAHC), medium-power-rated appliances of moderate cost (MPRAMC), and high-power-rated appliances of low cost (HPRALC). These load demands were assessed across multiple sectors, including community, residential, commercial, agricultural, and small-scale industrial. These load demands are depicted in Figure 3.

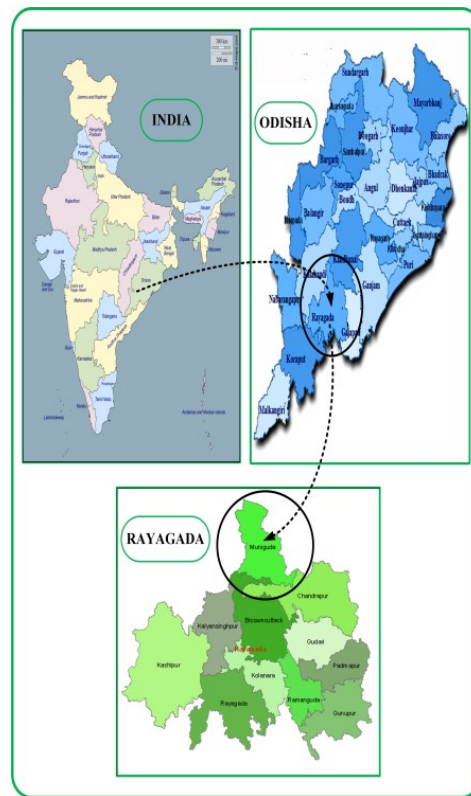


Figure 2. This study area’s location on a map.

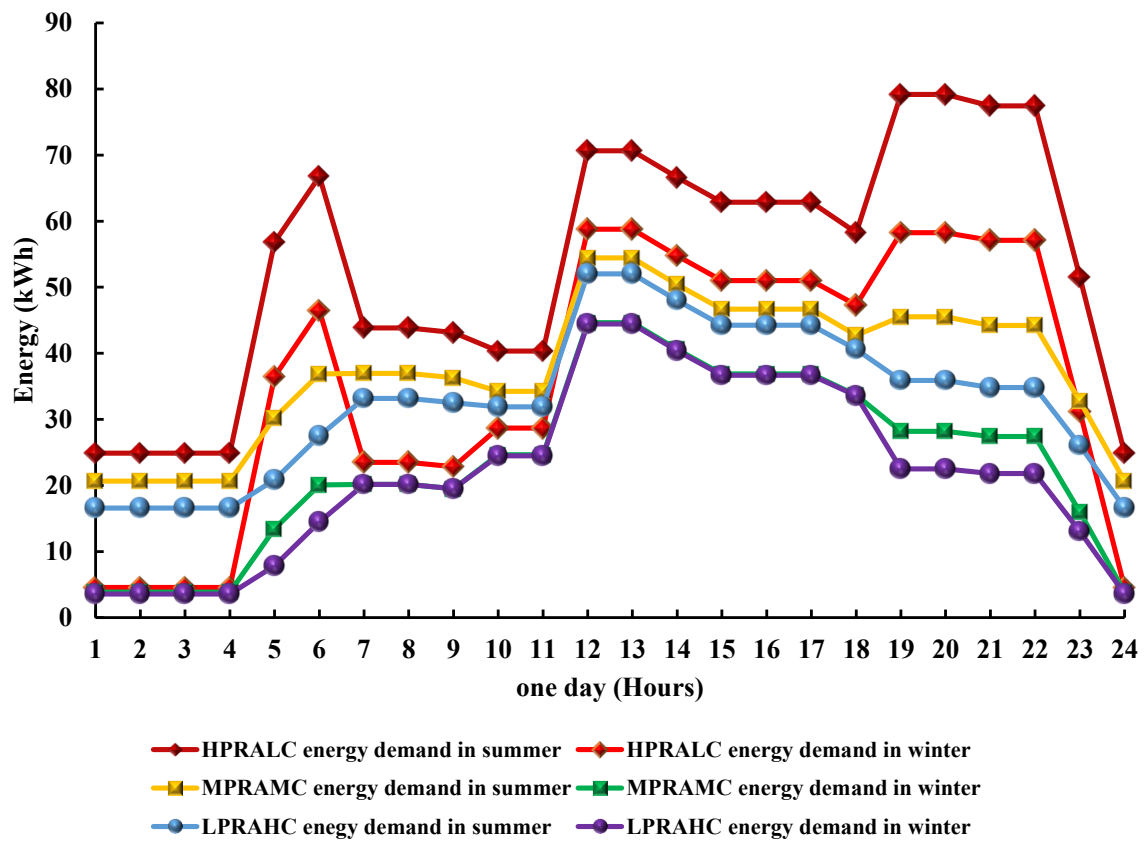


Figure 3. The seasonal variation in the hourly load demands for all scenarios during the winter and summer seasons.

Step 3—Resource assessment

Solar and biomass energy sources are the only renewable energy sources available in the study area. On average, the annual average of daily solar radiation is 5.18 kWh/m², while the temperature average is 26 °C celsius annually. Furthermore, 87 hectares of forest surround the location, which provides 60% of its foliage for collection. This foliage includes leaves, pine needles, and firewood, yielding approximately nine tons of biomass each year. Figures 4 and 5 are drawn using the data collected from the National Renewable Energy Laboratory to illustrate the hourly solar radiation and temperature trends from 2005–2015. These figures demonstrate the potential of these renewable energy sources in the study area.

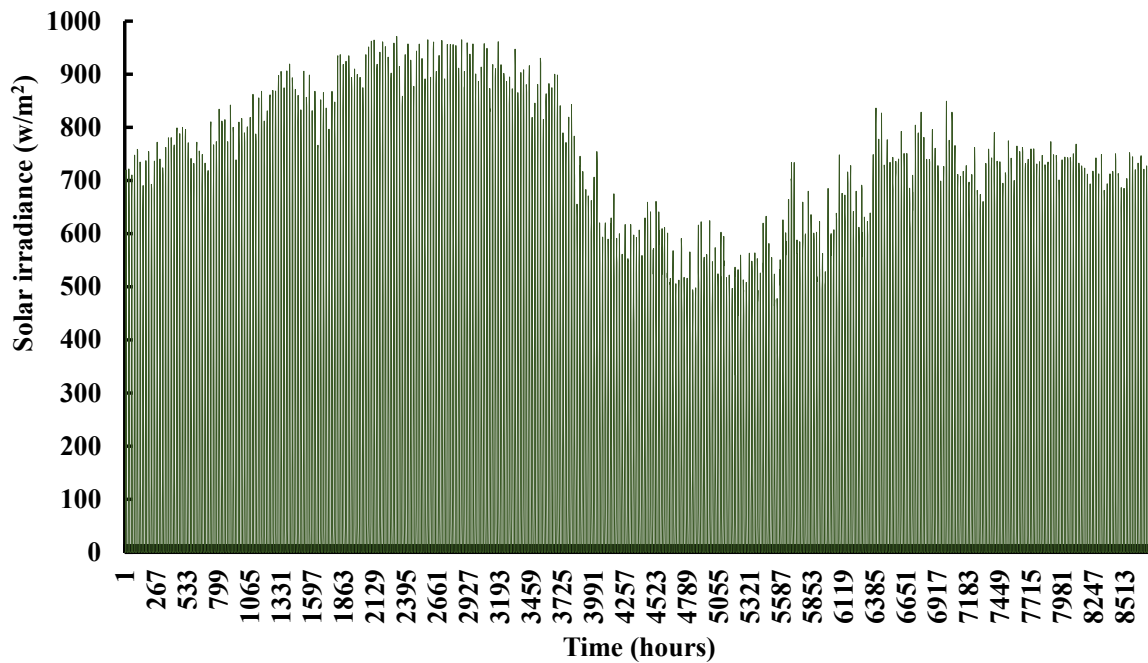


Figure 4. Annual solar radiation in the area under study.

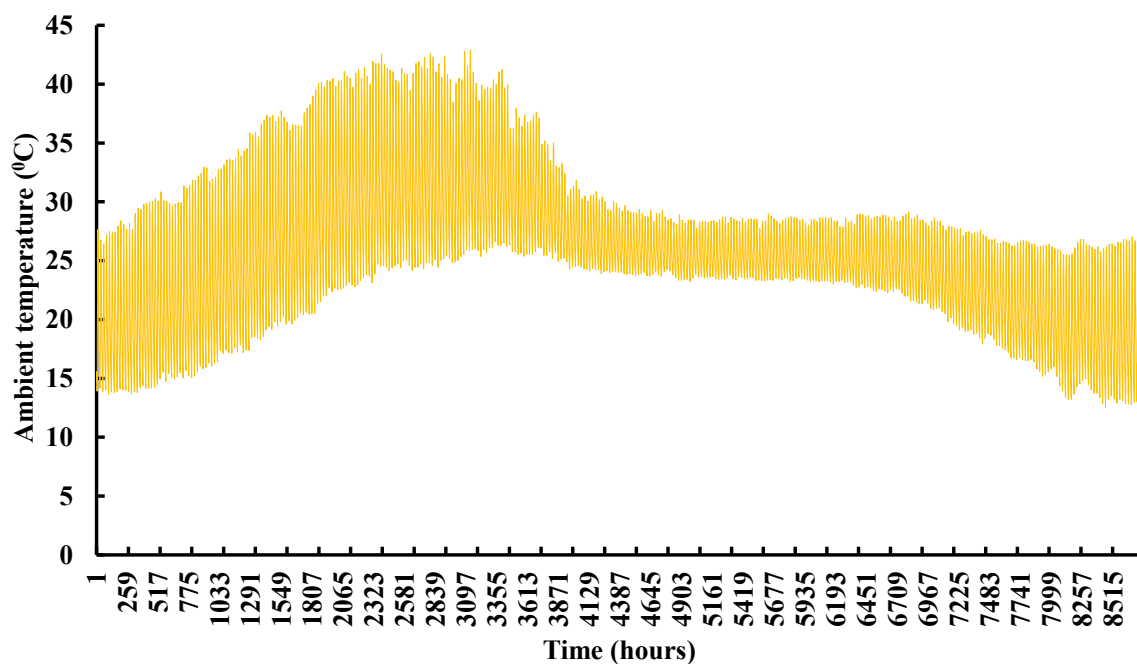


Figure 5. The annual ambient temperature in the area under study.

3. The IRES Component's Mathematical Modeling

The mathematical modeling of the components is explained below, as illustrated in Figure 6. The schematic diagram shows how the components work together to achieve the desired outcome.

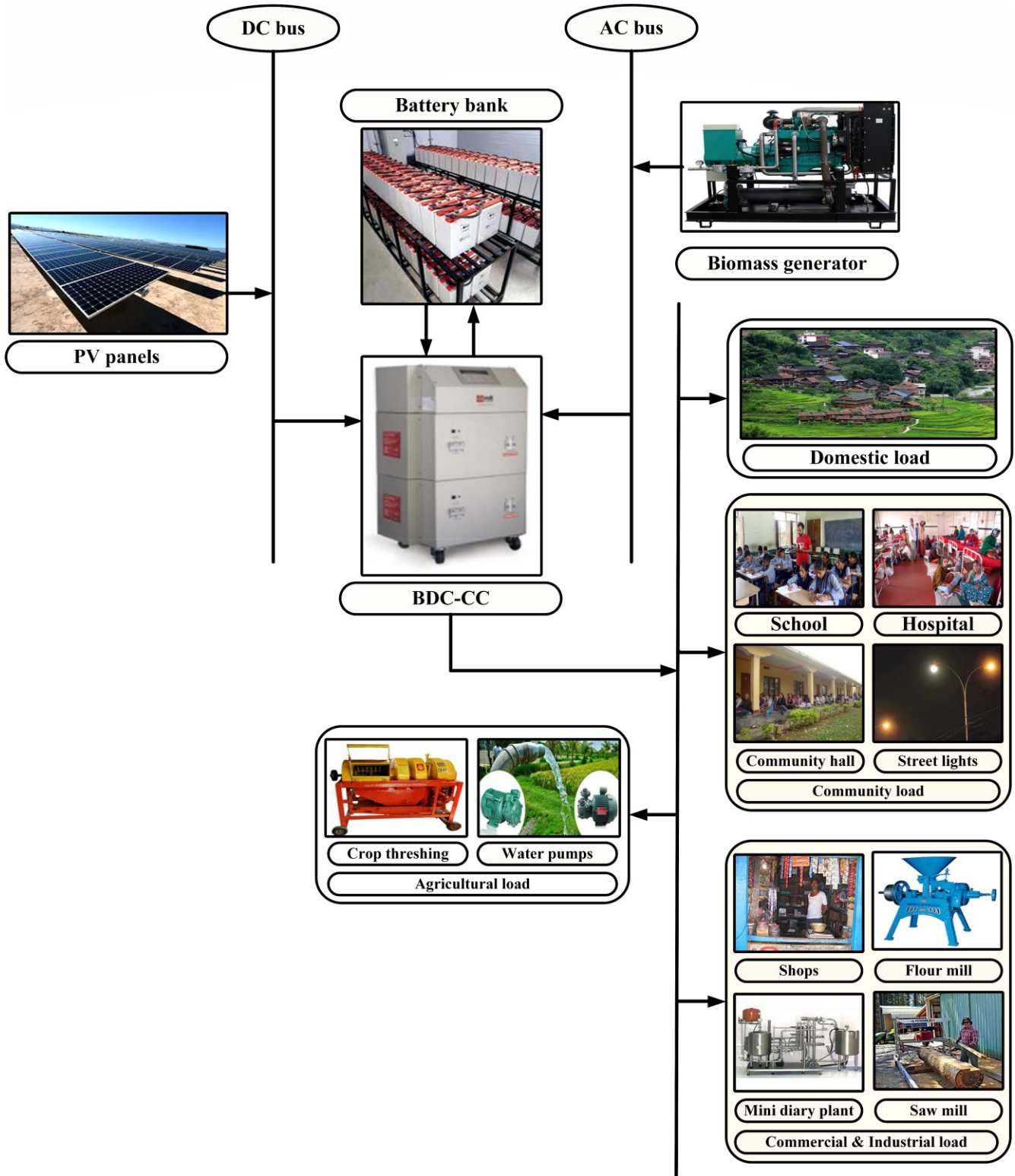


Figure 6. The IRES diagram.

3.1. Solar Energy

The output power generated by the solar PV panel is expressed as follows [2]:

$$P_{PV}(t) = PV_{rated} \times (G(t)/G_{ref}) \times \left[1 + K_T \times (T_C - T_{ref})\right] \quad (1)$$

To determine the temperature inside a solar cell, the following formula will be useful:

$$T_C = T_{amb}(t) + (0.0256 \times G(t)) \quad (2)$$

3.2. Biomass Generator

The following expression describes the Biomass Generator's output power [1]:

$$P_{BMG}(t) = \frac{Q_{BM} \times \eta_{BMG} \times CV_{BM} \times 1000}{DOH_{BMG} \times 365 \times 860} \quad (3)$$

3.3. Battery Bank

The following expression is useful for the battery bank charging [2,29]:

$$E_{Bat}(t) = (1 - \sigma) \times E_{Bat}(t - 1) + (E_G(t) - E_L(t)/\eta_{Conv}) \times \eta_{CC} \times \eta_{rbat} \quad (4)$$

The energy generated by the Renewable Energy resources is calculated as follows:

$$E_G(t) = [E_{DC}(t) + E_{AC}(t)] \times \eta_{Conv} \quad (5)$$

The DC energy produced by the Renewable Energy resources is expressed as follows:

$$E_{DC}(t) = E_{PV}(t) \quad (6)$$

The AC energy produced by the Renewable Energy resources is expressed as follows:

$$E_{AC}(t) = E_{BMG}(t) \quad (7)$$

The discharging of the battery bank is expressed as follows [4,5]:

$$E_{Bat}(t) = (1 - \sigma) \times E_{Bat}(t - 1) - (E_L(t)/\eta_{Conv} - E_G(t))/\eta_{rbat} \quad (8)$$

4. Economic Analysis of the IRES

The life-cycle cost of the system is calculated as follows [1]:

$$LCC = ICC + EREC + P_{V,O\&M} + P_{V,REP} + P_{V,FUEL} \quad (9)$$

The initial capital cost (ICC) is considered as follows [1]:

$$ICC = \left[(C_{BMG,cap}) + (N_{PV} \times C_{PV,cap}) + (N_{BAT} \times C_{BAT,cap}) + (C_{BDC-CC,cap}) + (C_{MEM,cap}) + (C_{WTA,cap}) + (C_{CHE,cap}) \right] \quad (10)$$

The erection is considered as follows [1]:

$$EREC = \left[(N_{PV} \times C_{PV,erect}) + \left((N_{BAT} \times C_{BAT,erect}) \times \sum_{b=1}^{N_r} \frac{(1+x)^{bN_c-1}}{(1+y)^{bN_c}} \right) + \left(C_{BDC-CC,erect} \times \sum_{d=1}^{N_r} \frac{(1+x)^{dN_c-1}}{(1+y)^{dN_c}} \right) + \left(C_{BMG,erect} \times \sum_{g=1}^{N_r} \frac{(1+x)^{gN_c-1}}{(1+y)^{gN_c}} \right) \right] \quad (11)$$

The O&M cost of the system is considered as follows [1]:

$$P_{V,O\&M} = \left[\begin{array}{l} (N_{PV} \times C_{PV,o\&m}) + (C_{BMG,o\&m}) \\ (N_{BAT} \times C_{BAT,o\&m}) + (C_{BDC-CC,o\&m}) \end{array} \right] \times \sum_{i=1}^N \frac{(1+x)^{i-1}}{(1+y)^i} \quad (12)$$

where y is defined as follows [1]:

$$y = \frac{I_{nom} - x}{1+x} \quad (13)$$

The replacement cost of the components is calculated as follows [1]:

$$P_{V,REP} = \left[\begin{array}{l} \left(N_{BAT} \times C_{BAT,rep} \times \sum_{b=1}^{N_r} \frac{(1+x)^{bN_c-1}}{(1+y)^{bN_c}} \right) + \left(C_{BMG,rep} \times \sum_{g=1}^{N_r} \frac{(1+x)^{gN_c-1}}{(1+y)^{gN_c}} \right) + \\ \left(C_{BDC-CC,rep} \times \sum_{d=1}^{N_r} \frac{(1+x)^{dN_c-1}}{(1+y)^{dN_c}} \right) \end{array} \right] \quad (14)$$

where N_r is defined as follows [1]:

$$N_r = int\left(\frac{N - N_c}{N_c}\right) \quad (15)$$

The fuel cost is considered as follows [1]:

$$P_{V,FUEL} = [(C_{BM} \times Q_{BM})] \times \sum_{i=1}^N \frac{(1+x)^{i-1}}{(1+y)^i} \quad (16)$$

5. The Objective Function and Its Constraints

The objective function of the system and its constraints are discussed as follows [1]:

5.1. Life-Cycle Cost

The objective function is considered as follows:

$$minLCC(N_{PV}, N_{BAT}) = \sum_{C=PV,BMG,BAT,ROD,BDC-CC}^{min} (LCC)_C \quad (17)$$

5.2. Upper and Lower Bounds

We assume a 5-kW biomass generator that operates throughout the evening peak demand period (6–10 p.m.) and produces 4 kWh of energy as part of our analysis.

The solar energy resource is constrained as follows:

$$0 \leq N_{PV} \leq N_{PV-max} \quad (18)$$

The following limitation applies to the battery bank:

$$0 \leq N_{BAT} \leq N_{BAT-max} \quad (19)$$

5.3. Battery Bank Energy Storage Limits

The energy that is stored in the battery bank is limited as follows [29]:

$$E_{Bat_min} \leq E_{Bat}(t) \leq E_{Bat_max} \quad (20)$$

The following calculation illustrates the range of the battery bank's energy storage capacity:

$$E_{Bat_max} = \left(\frac{N_{BAT} \times V_{BAT} \times S_{BAT}}{1000} \right) \times SOC_{max-bat} \quad (21)$$

$$E_{Bat_min} = \left(\frac{N_{BAT} \times V_{BAT} \times S_{BAT}}{1000} \right) \times SOC_{min-bat} \quad (22)$$

The minimum and maximum SOC of the battery bank is expressed as follows:

$$SOC_{min-bat} = 1 - DOD$$

$$SOC_{max-bat} = SOC_{min-bat} + DOD$$

5.4. Power Reliability Index

The Loss of Power Supply (LPS) of the system is expressed as follows [30–32]:

$$LPS(t) = \frac{E_L(t)}{\eta_{Conv}} - E_G(t) - [(1 - \sigma) \times E_{Bat}(t - 1) - E_{Bat_min}] \times \eta_{rbat} \quad (23)$$

The LPSP is calculated as follows [33]:

$$LPSP = \frac{\sum_{t=1}^T LPS(t)}{\sum_{t=1}^T E_L(t)} \quad (24)$$

6. Methodology

Mode 1: The amount of energy that can be produced by renewable energy sources surpasses the current demand. As a result, the batteries are charged using the excess energy generated from these renewable sources;

Mode 2: The load demand necessitates greater energy than what is available from renewable sources. For this reason, the battery provides adequate power to fulfill the requirements of the load;

Mode 3: The energy produced by renewable sources is sufficient to meet the needs of the load, and the batteries have already reached their max capacity. Therefore, the excess energy generated must be disposed of into the waste load;

Mode 4: The demand for power exceeds the energy generated by renewable sources, and the batteries are fully discharged, resulting in a loss of power supply.

7. Results and Discussions

The current study aimed to determine the best way to set up an IRES to meet the power needs of five distant communities in India's Odisha state. These communities are powered by such RE sources as biomass and solar. There is no guarantee that these RE sources will be available at all times; a consistent battery system is mandatory to ensure constant power generation. As a result, this study attempted to identify the most appropriate battery technology among the three battery technologies, lithium-ion, lead–acid, and nickel–iron, which would be the most technically and economically viable for the study area.

7.1. Various Configurations Using Battery Technologies and Renewable Energy Sources

For this study, models of three different lithium-ion battery configurations ("PV/BMG/Li-Ion@50% DOD, PV/BMG/Li-Ion@70% DOD, and PV/BMG/Li-Ion@80% DOD") have been created due to the versatility of lithium-ion batteries which can operate at various depths of discharge (DODs). Additionally, two lead–acid (LA) battery configurations, "PV/BMG/LA@70% DOD and PV/BMG/LA@80% DOD", have also been modeled in order to demonstrate the versatility of this technology. Additionally, the PV/BMG/Ni-Fe@80% DOD configuration was taken into account due to the fact that Ni-Fe batteries can operate at both @50% and @80% DOD with a 30-year or longer lifespan at both.

Using an HPRALC-based scenario (Without DSM) as a starting point, six different topologies are evaluated and compared in order to find the optimal configuration for bringing electricity to the area under investigation. This optimal configuration is then further evaluated by taking into account the demand side management (With DSM) in the MPRAMC and LPRAHC-based scenarios. Through this process, the most cost-effective and practicable configuration can be determined and implemented.

The Supplemental File includes information about the technical specifications and costs of this study's components, as well as the control parameters of the proposed algorithms.

7.2. The Optimal Configuration from the Lead–Acid Battery Technology

The lead–acid battery is modeled in two different configurations with 70% and 80% depth-of-discharge (DOD) settings. Using an HPRALC scenario, the optimal results for each configuration were determined, which are listed in Table 1. It was found that the lead–acid-battery-based IRES @80% DOD had the most financial viability, with an optimal LCC value of \$1,595,267, which was 2% less than the lead–acid-battery-based IRES @70% DOD. Furthermore, its optimal values for N_{PV} and $N_{BAT(LA)}$ were 1367 and 367, respectively. These results suggest that the lead–acid-battery-based IRES @80% DOD should be further explored in comparison to other battery-based IRESs.

Table 1. Optimization Results of the IRESs using HPRALC-based Scenario at an LPSP Value of 0%.

Configuration	Q&C	GA	PSO	DE	GWO	ALO	DA	MFO	GOA	SSA
PV/ BMG/ Ni–Fe @DOD = 80%	N_{PV}	1469	1469	1485	1469	1469	1469	1469	1469	1469
	N_{BAT}	950	950	962	950	950	950	950	950	950
	LCC (\$)	951,257	951,257	962,065	951,257	951,257	951,257	951,257	951,257	951,257
PV/ BMG/ LA @DOD = 70%	N_{PV}	1364	1364	1364	1422	1364	1364	1364	1364	1364
	N_{BAT}	420	420	420	422	420	420	420	420	420
	LCC (\$)	1,620,231	1,620,231	1,620,231	1,640,650	1,620,231	1,620,231	1,620,231	1,620,231	1,620,231
PV/ BMG/ LA @DOD = 80%	N_{PV}	1367	1367	1383	1367	1367	1367	1367	1367	1367
	N_{BAT}	367	367	369	367	367	367	367	367	367
	LCC (\$)	1,595,267	1,595,267	1,605,861	1,595,267	1,595,267	1,595,267	1,595,267	1,595,267	1,595,267
PV/ BMG/ Li-Ion @DOD = 50%	N_{PV}	1264	1264	1266	1264	1536	2000	1264	1264	1264
	N_{BAT}	419	419	420	419	411	398	419	419	419
	LCC (\$)	2,712,794	2,712,794	2,718,907	2,712,794	2,736,122	2,779,547	2,712,794	2,712,794	2,712,794
PV/ BMG/ Li-Ion @DOD = 70%	N_{PV}	1649	1268	1268	1268	1364	1730	1272	1242	1268
	N_{BAT}	291	299	299	299	297	290	300	300	299
	LCC (\$)	2,804,117	2,773,053	2,773,053	2,773,053	2,781,007	2,816,370	2,782,117	2,774,594	2,773,053
PV/ BMG/ Li-Ion @DOD = 80%	N_{PV}	1245	1354	1408	1245	1953	2000	1245	1245	1245
	N_{BAT}	262	260	259	262	249	249	262	262	262
	LCC (\$)	3,025,532	3,032,498	3,035,855	3,025,532	3,070,686	3,082,473	3,025,532	3,025,532	3,025,532

7.3. The Optimal Configuration from the Lithium-Ion Battery Technology

The lithium-ion battery has been configured with three different depths of discharge (DODs): 50%; 70%; and 80%. According to a comprehensive HPRALC-based analysis, the Li-Ion-battery-based IRES @50% DOD was determined to be the most financially viable option, boasting an optimal life-cycle cost (LCC) of \$1,595,267, which is 2% and 10% less than the optimal LCCs for lithium-ion-battery-based IRESs @70% and 80% DODs. Furthermore, the optimal N_{PV} and $N_{BAT(Li-Ion)}$ values for this configuration are 1264 and 419, respectively, which are listed in Table 1. Consequently, the lithium-ion-battery-based IRES @50% DOD has been taken into consideration for further comparisons with other battery-based IRESs.

7.4. The Optimal Configuration from the Nickel–Iron Battery Technology

The nickel–iron battery has a lifespan of more than 30 years at both DOD levels of 50% and 80%. For this reason, the research undertaken was only analyzed with a DOD of 80%. The results given in Table 1 show that the most cost-effective life-cycle cost (LCC) of an iron-based IRES with a DOD of 80% is \$951,257 when using an HPRALC-based scenario. This configuration features $N_{PV} = 1469$ and $N_{BAT(Ni-Fe)} = 950$ as its optimal component values.

7.5. Optimal Configuration from the HPRALC, MPRAMC, and LPRAHC-Based Configurations

Three different efficiency-based scenarios—“HPRALC”, “MPRAMC”, and “LPRAHC”—were analyzed in order to establish the optimum set for the system.”

7.5.1. The HPRALC-Based Scenario (without DSM)

Without DSM, the Ni–Fe-battery-based IRES @80% DOD (base case) provides the lowest life-cycle cost (LCC) of \$951,257 for the HPRALC-based scenario. Compared to this, the LA battery-based IRES provided an LCC of \$1,595,267 at 80% DOD, which is approximately 68% higher. If the IRES were powered by a lithium–ion battery at 50% DOD, its optimal life-cycle cost would be \$2,712,794, which is approximately 185% higher than the base case LCC. It is, thus, evident that nickel–iron batteries offer the most economical solution in this study area, followed by lead–acid and lithium-ion batteries. Therefore, they are omitted from additional analysis in Section 7.5.2 (MPRAMC-based scenario) and Section 7.5.3 (LPRAHC-based scenario).

7.5.2. Medium Efficiency Appliances Usage-Based Scenario (MPRAMC) (with DSM)

In the HPRALC scenario, the Ni–Fe-battery-based IRES (base case) was found to have the lowest LCC when compared to other battery-based IRESs. This configuration was then thoroughly examined using a scenario based on the use of appliances with an MPRAMC-based scenario (i.e., with DSM). The MPRAMC scenario describes a situation in which consumers use medium-power-rated appliances of moderate cost. Table 2 reveals that the LCC provided by the MPRAMC-based scenario is 33% lower than the base case LCC of the HPRALC-based scenario, i.e., \$635,271. Moreover, the optimal values of the N_{PV} and $N_{BAT(Ni-Fe)}$ components, in this case, are 1005 and 612, respectively. This demonstrates that the use of MPRAMC appliances has a remarkable effect on the system performance, resulting in a lower LCC and fewer components required when compared to the optimal values obtained using the HPRALC-based scenario.

Table 2. Optimization results of the IRESs using MPRAMC-based scenario at an LPSP Value of 0%.

Configuration	Q&C	GA	PSO	DE	GWO	ALO	DA	MFO	GOA	SSA
PV/	N_{PV}	1005	1005	1008	1005	1005	1005	1005	1005	1005
BMG/ Ni–Fe	N_{BAT}	612	612	625	612	612	612	612	612	612
@DOD = 80%	LCC (\$)	635,271	635,271	643,385	635,271	635,271	635,271	635,271	635,271	635,271

7.5.3. High-Efficiency Appliances Usage-Based Scenario (LPRAHC) (with DSM)

Based on the results of the HPRALC-based situation, it was determined that the nickel–iron-battery-based IRES (base case) offered the lowest LCC. As a result, we conducted additional research on this configuration using the LPRAHC-based scenario to gain further insights. Table 3 demonstrates that the LCC provided by the base case using HPRALC and MPRAMC-based scenarios and the LCC provided by the LPRAHC-based scenario is approximately 44% and 17% lower than the HPRALC and MPRAMC-based scenarios, respectively. For this case, the optimal values for the individual components are ($N_{PV} = 852$) and ($N_{BAT(Ni-Fe)} = 496$). When compared with the HPRALC-based scenario, the number of necessary PV panels is reduced by 617, from 1469 to 852, while the number of required batteries is decreased by 454, from 950 to 496. The scenario values from the MPRAMC

enabled us to reduce the number of PV panels from 1005 to 852, a decrease of 153 panels, and the number of batteries from 612 to 496, a drop of 116. The adoption of an LPRAHC-based scenario has a substantial impact on the system’s performance, as it reduces both the LCC and the number of components needed relative to the optimum values determined by the use of medium and low-efficiency appliances. Finally, it can be concluded that among various battery-based IRESs and efficiency-based scenarios, the LPRAHC-based scenario is the most suitable for electrifying the study area.

Table 3. Optimization results of the IRESs using LPRAHC-based scenario at an LPSP value of 0%.

Configuration	Q&C	GA	PSO	DE	GWO	ALO	DA	MFO	GOA	SSA
PV/	N _{PV}	852	852	852	852	852	852	852	852	852
BMG/ Ni-Fe	N _{BAT}	496	496	500	496	496	496	496	496	496
@DOD = 80%	LCC (\$)	530,603	530,603	532,868	530,603	530,603	530,603	530,603	530,603	530,603

Figures 7 and 8 show the energy graphs of the components of the IRES for one week throughout both the summer and winter months for the LPRAHC-based scenario of the nickel-iron-battery-based IRES.

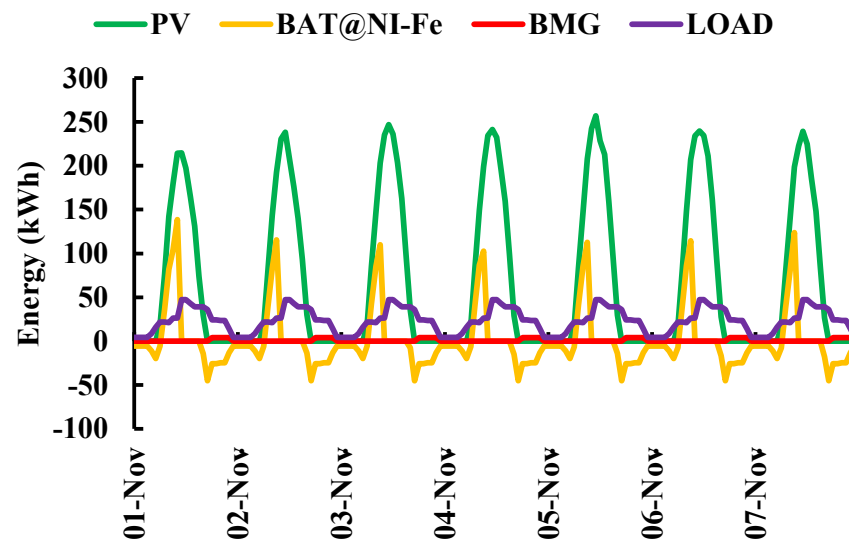


Figure 7. The energy outputs of the different components of the nickel-iron-battery-based IRES were measured over the course of one week in November during the winter season.

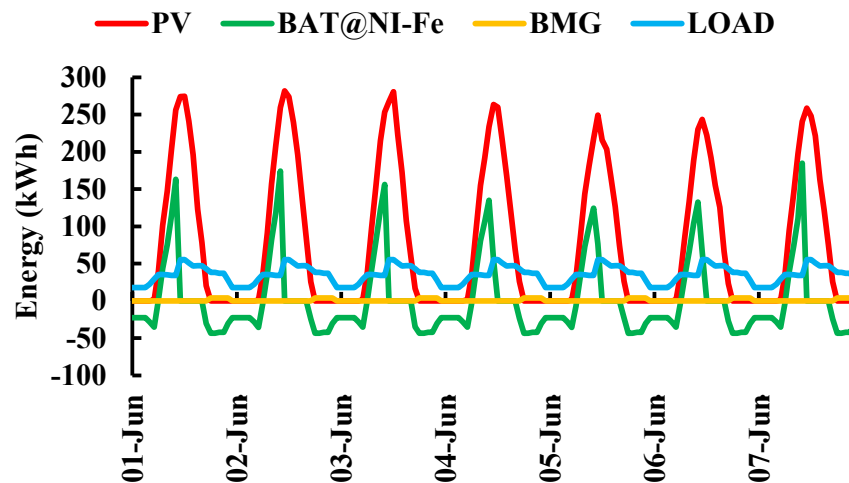


Figure 8. During the summer season of one week in June, the energy outputs of various components of the Ni-Fe-battery-based IRES.

7.6. The Algorithm's Ability to Find the Global Best Optimal Solutions

The results presented in Tables 1–3 for the three efficiency scenarios of eight configurations demonstrate that the SSA algorithm is the most robust, offering the global best optimal values for all configurations. The DE algorithm came in fourth, providing the global best optimal values for only two configurations. The ALO and DA algorithms ranked third, each providing the global best optimal values for five configurations. The GA, PSO, GWO, MFO, and GOA algorithms obtained a second place, as they provided the global best optimal values for seven configurations. Overall, the SSA algorithm clearly proved to be the most reliable in finding the global best optimal values.

7.7. The Algorithms' Effectiveness in Achieving the Global Best Optimal Solutions

Figure 9 presents the convergence curves of the various algorithms used to analyze nickel–iron-based IRES@80% DOD with an HPRALC-based scenario. The lowest possible LCC is achieved by GA, PSO, GWO, ALO, DA, MFO, GOA, and SSA algorithms at the 28th, 48th, 69th, 36th, 63rd, 61st, 94th, and 15th iterations, respectively.

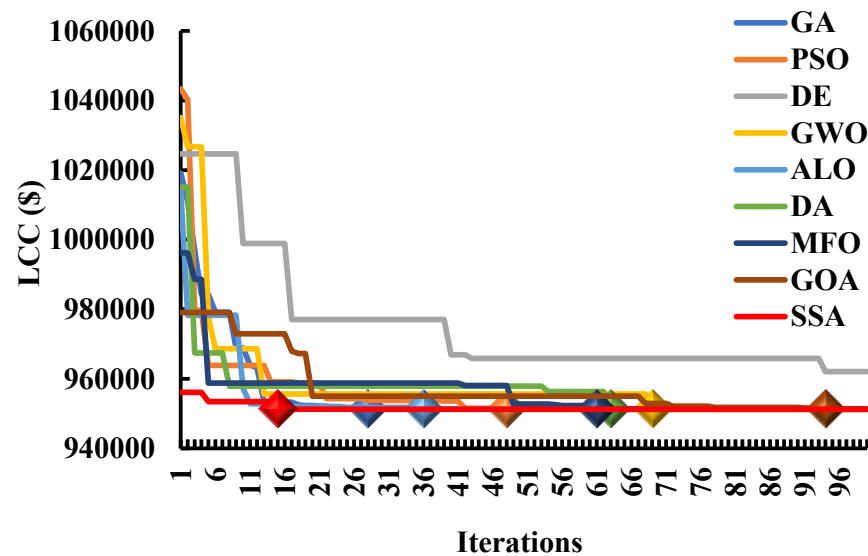


Figure 9. IRES powered by Ni–Fe batteries, complete with an HPRALC scenario and their respective convergence curves.

Figure 10 shows the converging curves of all algorithms for the LA-based IRES at 80% DOD with the HPRALC-based scenario. The GA, PSO, GWO, ALO, DA, MFO, GOA, and SSA algorithms yielded the least LCC values on the 38th, 52nd, 61st, 33rd, 66th, 56th, 93rd, and 25th iterations, respectively.

The convergence curves of all algorithms used for an HPRALC-based scenario on the lithium-ion IRES at 50% DOD are presented in Figure 11. The GA, PSO, GWO, MFO, GOA, and SSA algorithms achieved the lowest LCCs at the 61st, 54th, 93rd, 42nd, 82nd, and 29th iterations, respectively.

The convergence curves of all techniques for a nickel–iron-battery-based IRES operating at 80% DOD with an MPRALC-based scenario are depicted in Figure 12. The GA, PSO, GWO, ALO, DA, MFO, and SSA algorithms had the lowest LCC at the 28th, 59th, 95th, 30th, 81st, 93rd, and 23rd iterations, respectively.

Figure 13 shows the convergence curves of the nickel–iron-battery-based IRES with an LPRALC-based situation at 80% DOD. The minimum LCC of this configuration was obtained at the 32nd, 29th, 96th, 59th, 64th, 26th, 91st, and 21st iterations using the GA, PSO, GWO, ALO, DA, MFO, GOA, and SSA algorithms, respectively.

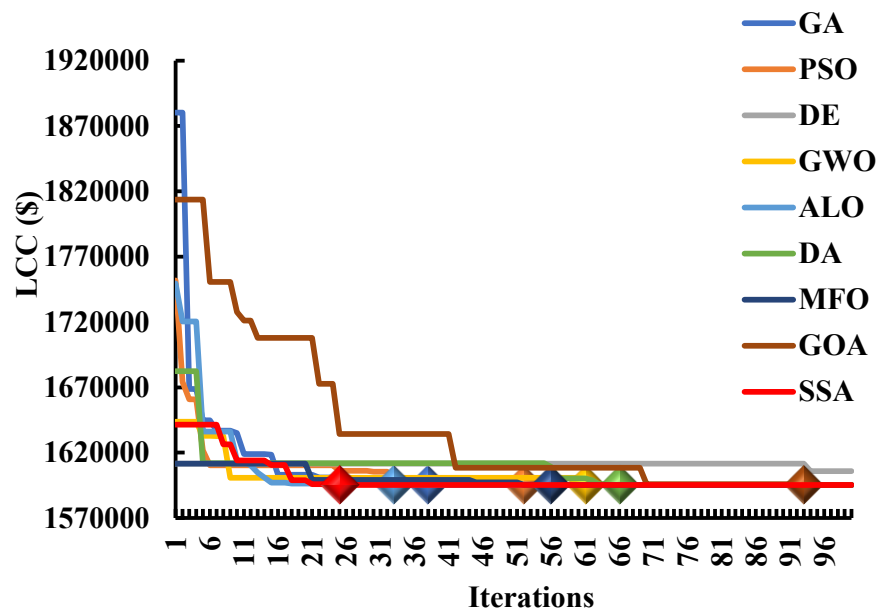


Figure 10. Curves of convergence for the lead-acid-battery-based IRES under the conditions of HPRALC.

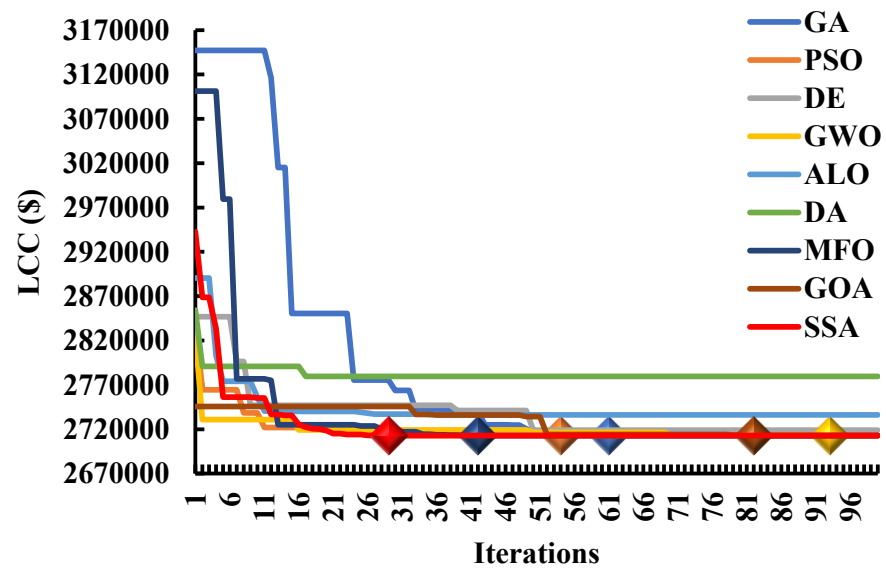


Figure 11. Curves of convergence for the IRES powered by Li-Ion batteries in the HPRALC scenario.

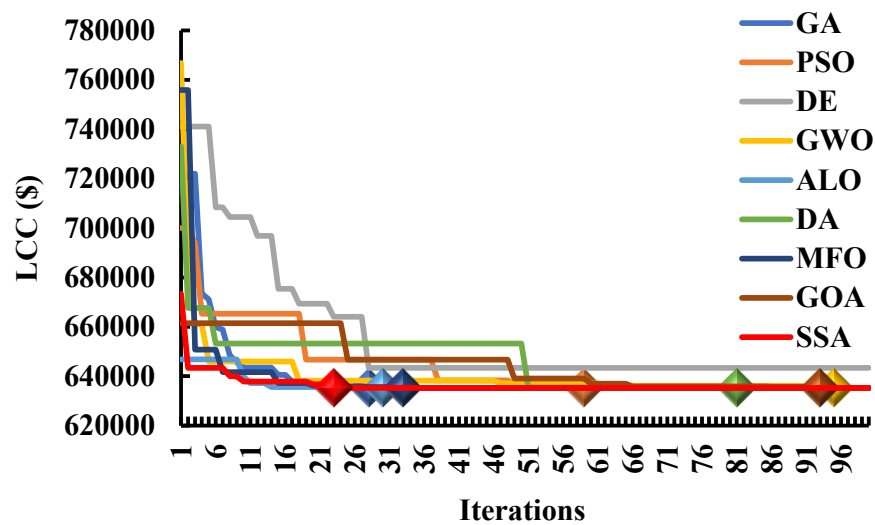


Figure 12. Curves of convergence for the nickel–iron-battery-based IRES with the MPRAMC scenario.

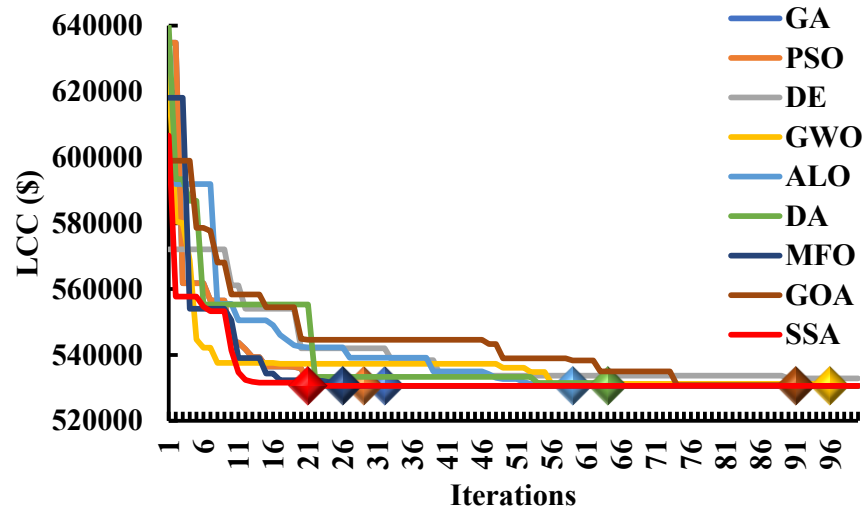


Figure 13. Convergence curves of the Ni–Fe-battery-based IRES with LPRAHc scenario.

The proposed SSA algorithm has been demonstrated to be reliable and efficient in achieving the global best optimal values for all efficiency-based scenarios, as evidenced in Sections 7.6 and 7.7. Consequently, it is recommended for use in addressing all microgrid size issues.

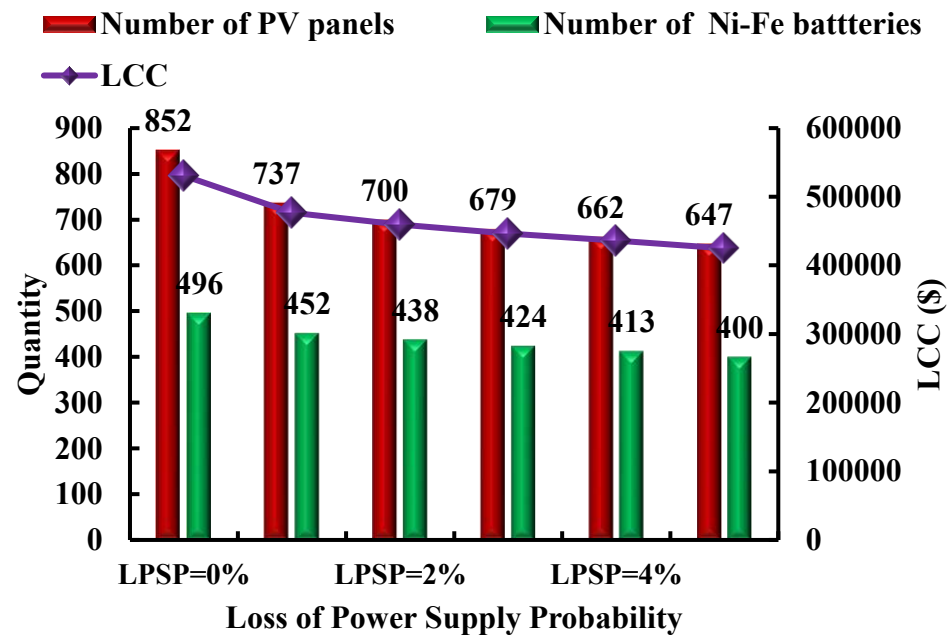
7.8. The Impact of LPSP on the System Efficiency

The Ni–Fe-battery-based IRES with the LPRAHc-based scenario was identified as the optimal configuration for the electrification of the study area at 0% LPSP. The proposed SSA algorithm was used to analyze this optimal configuration over a range of LPSP values from 0 to 5%, and the results are presented in Table 4.

Table 4 and Figure 14 show a significant difference in optimal values obtained with 0% and 1% loss of power supply probability values. The LCC value is reduced by 10%; the number of Photovoltaic (PV) panels is reduced from 852 to 737, and the number of batteries is reduced from 496 to 452 when a 1% LPSP value is assumed. With 1% power loss, the total number of power lost hours is only 173 out of 8760. Furthermore, increasing the LPSP values from 2% to 5% further reduces the achieved LCCs and component values, but with a small increase in the number of lost power hours. Hence, the Ni–Fe-battery-based IRES with an LPSP value of 1% can be used to provide power supply to the study area with notable cost savings at minimal loss of power hours when compared to the optimal values at 0% LPSP.

Table 4. The results of the optimal configuration at different LPSP values.

Configuration	Quantity and Cost	LPSP (0%)	LPSP (1%)	LPSP (2%)	LPSP (3%)	LPSP (4%)	LPSP (5%)
PV/ BMG/ Ni-Fe @DOD = 80%	N _{PV}	852	737	700	679	662	647
	N _{BAT}	496	452	438	424	413	400
	LCC (\$)	530,603	476,846	459,639	446,445	435,953	424,829
	LPSH	0	173	310	467	579	649

**Figure 14.** Variability in LCC and related components at various LPSP values.

8. Conclusions

The optimal design for electrifying the study area has been determined by modeling six different configurations that leveraged renewable energy resources and battery technologies. These configurations include PV/BMG/LA at 70% depth of discharge (DOD), PV/BMG/LA at 80% DOD, PV/BMG/Li-Ion at 50% DOD, PV/BMG/Li-Ion at 70% DOD, PV/BMG/Li-Ion at 80% DOD, and PV/BMG/Ni-Fe at 80% DOD. The analysis of these configurations is necessary to identify the most cost-effective and efficient solution for the study area. Nine metaheuristic algorithms, such as particle swarm optimization, grey wolf optimization, genetic algorithm, ant lion optimization, differential evolutionary algorithm, moth flame optimization, dragonfly algorithm, grasshopper optimization algorithm, and salp swarm algorithms, were assessed in a MATLAB environment under a scenario of low-efficiency appliances usage-based scenario. Our research showed that the salp swarm algorithm is an efficient and reliable one for finding the global best optimal values. Our study revealed that this algorithm is capable of providing effective solutions quickly and accurately. The Ni-Fe-battery-based IRES has been found to be an optimal configuration with a low-efficiency-appliance usage-based scenario, which was further evaluated with both medium and high-efficiency-appliance usage-based scenarios. The results indicate that the Ni-Fe-battery-based IRES is the optimal choice in all scenarios. The summary of these results is listed as follows:

- The Ni-Fe-battery-based IRES with low-efficiency-appliance usage-based scenario obtained a life-cycle cost (LCC) of \$951,257, which was 40% and 65% lower than the LA (@80% DOD) and lithium-ion (@50% DOD) battery-based IRESs LCCs, respectively;

- The Ni–Fe-battery-based IRES with medium-efficiency appliance usage-based scenario, i.e., with demand side management (DSM), yielded an LCC of \$635,271, which was 33% lower than its LCC when using the low-efficiency appliance usage-based scenario;
- The Ni–Fe-battery-based IRES system with the integration of high-efficiency appliance usage-based scenario, i.e., with DSM, led to a significant decrease in the LCC by 44% and 17% when compared to the scenarios based on low and medium-efficiency appliance usage-based scenarios, respectively, to \$530,603;
- This study determined that the Ni–Fe-battery-based IRES with DSM was the most cost-effective and efficient system for the study area. Future research should explore other renewable energy sources, control strategies, and innovative energy storage technologies in order to optimize the design of renewable energy-based systems.

Supplementary Materials: The following supporting information can be downloaded at <https://www.mdpi.com/article/10.3390/su151310137/s1>.

Author Contributions: Conceptualization, P.P.K. and R.S.S.N.; methodology, S.A.S. and M.F.I.; software, P.P.K. and R.S.S.N.; validation, S.M.M. and G.M.S.; formal analysis, M.F.I.; investigation, S.A.S., S.M.M. and A.R.; resources, S.A.S., A.R.; data curation, S.A.S., M.F.I., G.M.S. and A.R.; writing—original draft preparation, P.P.K. and R.S.S.N.; writing—review and editing, S.A.S., S.M.M. and G.M.S., I.C.; visualization, M.A.H., F.A. and R.M.E.; supervision, S.M.M.; project administration, S.A.S., M.A.H., F.A. and R.M.E., I.C.; funding acquisition, I.C. All authors have read and agreed to the published version of the manuscript.

Funding: This work received no external funding.

Institutional Review Board Statement: Not applicable.

Informed Consent Statement: Not applicable.

Data Availability Statement: Not applicable.

Acknowledgments: This work was supported by the Researchers Supporting Project number (RSPD2023R646), King Saud University, Riyadh, Saudi Arabia.

Conflicts of Interest: The authors declare no conflict of interest.

References

1. Patel, A.M.; Singal, S.K. Optimal component selection of integrated renewable energy system for power generation in stand-alone applications. *Energy* **2019**, *175*, 481–504. [\[CrossRef\]](#)
2. Bukar, A.L.; Tan, C.W.; Lau, K.Y. Optimal sizing of an autonomous photovoltaic/wind/battery/diesel generator microgrid using grasshopper optimization algorithm. *Sol. Energy* **2019**, *188*, 685–696. [\[CrossRef\]](#)
3. Kumar, P.P.; Saini, R.P. Optimization of an off-grid integrated hybrid renewable energy system with different battery technologies for rural electrification in India. *J. Energy Storage* **2020**, *32*, 101912. [\[CrossRef\]](#)
4. Bukar, A.L.; Tan, C.W. A review on stand-alone photovoltaic-wind energy system with fuel cell: System optimization and energy management strategy. *J. Clean. Prod.* **2019**, *221*, 73–88. [\[CrossRef\]](#)
5. Sinha, S.; Chandel, S. Review of software tools for hybrid renewable energy systems. *Renew. Sustain. Energy Rev.* **2014**, *32*, 192–205. [\[CrossRef\]](#)
6. Mirjalili, S.; Gandomi, A.H.; Mirjalili, S.Z.; Saremi, S.; Faris, H.; Mirjalili, S.M. Salp Swarm Algorithm: A bio-inspired optimizer for engineering design problems. *Adv. Eng. Softw.* **2017**, *114*, 163–191. [\[CrossRef\]](#)
7. Zia, M.F.; Elbouchikhi, E.; Benbouzid, M.; Guerrero, J.M. Energy Management System for an Islanded Microgrid with Convex Relaxation. *IEEE Trans. Ind. Appl.* **2019**, *55*, 7175–7185. [\[CrossRef\]](#)
8. Ramesh, M.; Saini, R.P. Dispatch strategies based performance analysis of a hybrid renewable energy system for a remote rural area in India. *J. Clean. Prod.* **2020**, *259*, 120697. [\[CrossRef\]](#)
9. Kim, H.; Jung, T.Y. Independent solar photovoltaic with Energy Storage Systems (ESS) for rural electrification in Myanmar. *Renew. Sustain. Energy Rev.* **2018**, *82*, 1187–1194. [\[CrossRef\]](#)
10. Kaabeche, A.; Bakelli, Y. Renewable hybrid system size optimization considering various electrochemical energy storage technologies. *Energy Convers. Manag.* **2019**, *193*, 162–175. [\[CrossRef\]](#)
11. Ayeng'O, S.P.; Schirmer, T.; Kairies, K.-P.; Axelsen, H.; Sauer, D.U. Comparison of off-grid power supply systems using lead-acid and lithium-ion batteries. *Sol. Energy* **2018**, *162*, 140–152. [\[CrossRef\]](#)
12. Li, C.; Zhou, D.; Wang, H.; Lu, Y.; Li, D. Techno-economic performance study of stand-alone wind/diesel/battery hybrid system with different battery technologies in the cold region of China. *Energy* **2020**, *192*, 116702. [\[CrossRef\]](#)

13. Farinis, G.; Kanellos, F.D. Integrated energy management system for Microgrids of building prosumers. *Electr. Power Syst. Res.* **2021**, *198*, 107357. [[CrossRef](#)]
14. Boglou, V.; Karavas, C.; Karlis, A.; Arvanitis, K. An intelligent decentralized energy management strategy for the optimal electric vehicles' charging in low-voltage islanded microgrids. *Int. J. Energy Res.* **2022**, *46*, 2988–3016. [[CrossRef](#)]
15. Zarate-Perez, E.; Rosales-Asensio, E.; González-Martínez, A.; de Simón-Martín, M.; Colmenar-Santos, A. Battery energy storage performance in microgrids: A scientific mapping perspective. *Energy Rep.* **2022**, *8*, 259–268. [[CrossRef](#)]
16. Boglou, V.; Karavas, C.-S.; Karlis, A.; Arvanitis, K.G.; Palaiologou, I. An Optimal Distributed RES Sizing Strategy in Hybrid Low Voltage Networks Focused on EVs' Integration. *IEEE Access* **2023**, *11*, 16250–16270. [[CrossRef](#)]
17. Rimpas, D.; Kaminaris, S.D.; Piromalis, D.D.; Vokas, G.; Arvanitis, K.G.; Karavas, C.-S. Comparative Review of Motor Technologies for Electric Vehicles Powered by a Hybrid Energy Storage System Based on Multi-Criteria Analysis. *Energies* **2023**, *16*, 2555. [[CrossRef](#)]
18. Huang, S.-C.; Lo, S.-L.; Lin, Y.-C. Application of a fuzzy cognitive map based on a structural equation model for the identification of limitations to the development of wind power. *Energy Policy* **2013**, *63*, 851–861. [[CrossRef](#)]
19. Karavas, C.-S.; Kyriakarakos, G.; Arvanitis, K.G.; Papadakis, G. A multi-agent decentralized energy management system based on distributed intelligence for the design and control of autonomous polygeneration microgrids. *Energy Convers. Manag.* **2015**, *103*, 166–179. [[CrossRef](#)]
20. Kokkinos, K.; Karayannis, V.; Moustakas, K. Circular bio-economy via energy transition supported by Fuzzy Cognitive Map modeling towards sustainable low-carbon environment. *Sci. Total Environ.* **2020**, *721*, 137754. [[CrossRef](#)]
21. Kennedy, J.; Eberhart, R. Particle Swarm Optimization. In Proceedings of the ICNN'95—International Conference on Neural Networks, Perth, Australia, 27 November–1 December 1995; pp. 1942–1948.
22. Storn, R.; Price, K. Differential evolution—A simple and efficient heuristic for global optimization over continuous spaces. *J. Glob. Optim.* **1997**, *11*, 341–359. [[CrossRef](#)]
23. Man, K.F.; Tang, K.S.; Kwong, S. Genetic algorithms: Concepts and applications [in engineering design]. *IEEE Trans. Ind. Electron.* **1996**, *43*, 519–534. [[CrossRef](#)]
24. Mirjalili, S. The Ant Lion Optimizer. *Adv. Eng. Softw.* **2015**, *83*, 80–98. [[CrossRef](#)]
25. Saremi, S.; Mirjalili, S.; Lewis, A. Grasshopper Optimisation Algorithm: Theory and application. *Adv. Eng. Softw.* **2017**, *105*, 30–47. [[CrossRef](#)]
26. Mirjalili, S.; Mirjalili, S.M.; Lewis, A. Grey Wolf Optimizer. *Adv. Eng. Softw.* **2014**, *69*, 46–61. [[CrossRef](#)]
27. Mirjalili, S. Moth-flame optimization algorithm: A novel nature-inspired heuristic paradigm. *Knowl. Based Syst.* **2015**, *89*, 228–249. [[CrossRef](#)]
28. Mirjalili, S. Dragonfly algorithm: A new meta-heuristic optimization technique for solving single-objective, discrete, and multi-objective problems. *Neural Comput. Appl.* **2016**, *27*, 1053–1073. [[CrossRef](#)]
29. Chauhan, A.; Saini, R. Discrete harmony search based size optimization of Integrated Renewable Energy System for remote rural areas of Uttarakhand state in India. *Renew. Energy* **2016**, *94*, 587–604. [[CrossRef](#)]
30. Lucchi, E. Integration between photovoltaic systems and cultural heritage: A socio-technical comparison of international policies, design criteria, applications, and innovation developments. *Energy Policy* **2022**, *171*, 113303. [[CrossRef](#)]
31. Lucchi, E.; Baiani, S.; Altamura, P. Design criteria for the integration of active solar technologies in the historic built environment: Taxonomy of international recommendations. *Energy Build.* **2023**, *278*, 112651. [[CrossRef](#)]
32. Lucchi, E. Renewable Energies and Architectural Heritage: Advanced Solutions and Future Perspectives. *Buildings* **2023**, *13*, 631. [[CrossRef](#)]
33. Maleki, A. Design and optimization of autonomous solar-wind-reverse osmosis desalination systems coupling battery and hydrogen energy storage by an improved bee algorithm. *Desalination* **2018**, *435*, 221–234. [[CrossRef](#)]

Disclaimer/Publisher's Note: The statements, opinions and data contained in all publications are solely those of the individual author(s) and contributor(s) and not of MDPI and/or the editor(s). MDPI and/or the editor(s) disclaim responsibility for any injury to people or property resulting from any ideas, methods, instructions or products referred to in the content.